Wholistic simulation of an all-electric refrigerated delivery vehicle

Agnes Poks[1†], Elisabeth Luchini[1], Filip Kitanoski[2] and Martin Kozek[1]

[1]Institute of Mechanics and Mechatronics Division of Control and Process Automation Getreidemarkt 9/325-A5, A-1060 Vienna, Austria
(Tel: +43-1-58801-325527; E-mail: agnes.poks@tuwien.ac.at)
[2]PRODUCTBLOKS GmbH, Stockerauer Str. 106, A-2100 Korneuburg, Austria

Abstract: Large amounts of goods have to be discarded because of a disrupted cooling chain, where last mile delivery is often the crucial part. For future refrigerated trucks which are fully electrified the limited battery capacity calls for detailed investigations. The main contribution of this paper is a detailed model of such an electric truck together with an electric cooling unit, which covers both the power consumption of the drive train and the cooling unit for various driving conditions. The proposed simulation framework is parameterized using measured data from literature, it comprises different weather conditions, door openings, traffic volume as well as the driver aggressiveness. The simulation model uses a minimum number of parameters for an easy fit, and due to it computational efficiency it can be used for applications like model predictive control.

Keywords: electric vehicles, refrigeration system, energy consumption

1. INTRODUCTION

The big metropolises consume over 80% of the global energy production and produce nearly the same amount of CO_2 emissions. The European Commission aims to reduce the CO_2 emission around 20% by end of 2020 and as long-term goal to reach by 2050 a CO_2 free transport sector that uses alternative and sustainable sources, [1]. In addition, approximately 50% of perishable produces, such as fruit, meat or medicine, must be disposed because of an interrupted cooling chain. Different solutions to this problem have been proposed, one of them being refrigerated transporters [2], [3], where both the drive-train, the auxiliaries, and the refrigeration system are electrically powered. However, this technology faces a number of challenges, in particular the limitation of the battery capacity in combination with the energy consumption for the vehicle, auxiliaries and especially the refrigeration unit.

A tool to design the battery that uses standardized drive cycles and a generic EV is based on published vehicle parameter is shown in [4]. The tool includes the EV model and a battery model but the standardized drive cycles don't comply with individual delivery route. The environment conditions are not modeled in this work and neither is a refrigeration cargo box (CB) included. A similar approach was done in [5] and [6]. The first uses various driving cycles to get an understanding of the vehicle power train and to develop a vehicle model. The second explores the sensitivity of the vehicle model according to the driver model. Both papers are based on the standardized cycles and designed for vehicles without a refrigeration system. Another work considers dedicated driving cycles which are based on real tracking information to improve the accuracy of the model, [7]. The designed model is based on small EVs without a refrigeration box. An approach for model predictive temperature control for a refrigerated vehicle was modeled in [8]. The cited paper focused on non-measurable disturbances like the aging of the thermal insulation and solar irradiation. Another paper reviews the work that has been carried out specifically on the modeling of food temperature, [9]. However, the cited papers consider conventional trucks without consumption of the engine.

In contrast to the previous references this contribution considers both, the consumption of the electrical drive and the electrical refrigeration unit. Moreover, several additional simulation parameters allow for a flexible simulation setup. A simulation framework for the energy consumption of an electrical vehicle with refrigeration unit is developed. The model of the electrical vehicle is validated with real measurements of comparable electrical vehicles, [10], and using published electrical vehicle parameters, [11]. It is shown that the framework includes the effects of both traffic density and driver characteristics and that the influence of delivery route, geographic and weather data is also incorporated. This allows an accurate simulation for the energy consumption for all three main consumers. The main contribution is the combination of several model components with similar complexity. The resulting simulation framework is therefore computationally efficient and the effect of design changes of major components becomes transparent.

The remainder of the paper is structured as follows: In Section 2 the model of the electrical vehicle is explained. Furthermore, the method to design the customized driving cycles is presented that considers the traffic situation as well as the driver characteristic. In Section 3 the refrigeration box for the vehicle and the disturbances are explained. Simulation results are shown in Section 4 and a short conclusion finalizes the paper.

2. VEHICLE MODELING

The energy consumption of the vehicle is caused by the longitudinal dynamic resistances. Also, partly the

† Agnes Poks is the presenter of this paper.

auxiliary consumers affect the total energy consumption of the vehicle depending on seasons. The necessary equations and relationships to build the model and to perform the validation through real measurements will be discussed in this Section.

2.1. Longitudinal vehicle model

The longitudinal dynamics description for a vehicle model without lateral influences is utilized here, [12]. The components which are considered in this model are:

- acceleration force F_{acc}
- friction force (tires) F_{fric}
- air drag force F_{drag}
- slope force F_{sl}

The vehicle is assumed to be one mass point m, its equation of motion can be written as follows:

$$m\dot{v} = F_{\text{acc}} - F_{\text{fric}} - F_{\text{drag}} - F_{\text{sl}}, \tag{1}$$

where $\dot{v}$ is the resulting vehicle acceleration. In Fig. 1 the longitudinal vehicle model with forces described in Eq. (1) is shown:

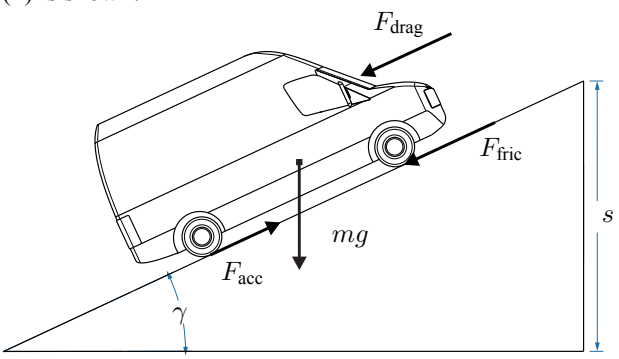

Fig. 1 Forces in the dynamic model of the electric vehicle.

For a given speed profile $v(t)$ the acceleration force F_{acc} follows to

$$F_{\text{acc}}(v(t)) = F_{\text{fric}} + F_{\text{drag}}(v(t)) + F_{\text{sl}} + m\dot{v}(t). \tag{2}$$

The aerodynamic drag force $F_{\text{drag}}(v(t))$ is defined through the equation

$$F_{\text{drag}}(v(t)) = \tfrac{1}{2}\rho A_f c_d v(t)^2, \tag{3}$$

where c_d is the drag coefficient, A_f the frontal area of the vehicle, ρ the density of the air and v the velocity of the car. In this model a simple rolling resistance description is used, [13]. The rolling resistance is given by

$$F_{\text{fric}} = 1.25 mg c_r, \tag{4}$$

where c_r is the constant rolling resistant coefficient and g the acceleration due to gravity. The slope force is the horizontal component of the vehicle mass when the vehicle is moving uphill or downhill with the angle γ

$$F_{\text{sl}} = mg\sin(\gamma) = mg\sin(\arctan(s)), \tag{5}$$

where the height difference of the surface is expressed in percent of the slope s. The mechanical power P_{mech} required to follow the speed profile $v(t)$ is given by

$$P_{\text{mech}}(v(t)) = F_{\text{acc}}(v(t))v(t). \tag{6}$$

The electrical power P_{el} is computed using

$$P_{\text{el}}(v(t)) = \frac{1}{\eta_{\text{el}}} P_{\text{mech}}(v(t)), \tag{7}$$

where $\eta_{\text{el}} < 1$ is the efficiency of the electric drive train and battery.

The energy consumption since the start of the route is given by

$$W_{\text{el}} = \int_0^t P_{\text{el}}\, d\tau. \tag{8}$$

2.2. Driving characteristics

A common approach to model the driver characteristics is using a standardized driving cycle, The New European Driving Cycle (NEDC), [14], and a transfer function that describes the driver aggressiveness, [4]. To create individual driving cycles with customized characteristics a model which calculates local speed variations in trapezoidal shape is used. Fig. 2 shows such a trapezoidal speed variation.

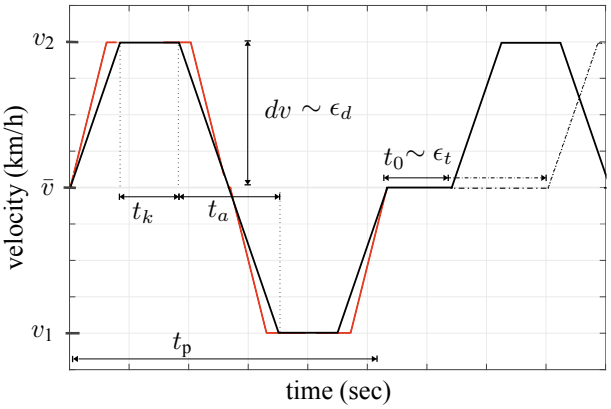

Fig. 2 Local speed variation with trapezoidal shape

The velocity profile of the trapezoid begins at $\bar{v}$ and then accelerates to v_2. After time t_k the speed is reduced to v_1. Again after time t_k the speed accelerates back to $\bar{v}$. The amplitude of the acceleration/deceleration depends on the parameter dv. The minimum and maximum velocity is calculated with the following equations:

$$\begin{aligned} v_1 &= (\bar{v} - \bar{v}dv) \\ v_2 &= (\bar{v} + \bar{v}dv) \end{aligned}$$

For the definition of the de- and acceleration time t_a, the maximum acceleration of the vehicle $\dot{v}_{\text{max}}$ multiplied with the parameter ϵ_d is used. The parameter ϵ_d describes the driver aggressiveness and directly influences the gradient of the trapezoid and the time t_a:

$$\begin{aligned} t_{\text{a}} &= \frac{v_2 - v_1}{\epsilon_d \dot{v}_{\text{max}}}, \\ t_{\text{p}} &= \frac{t_{\text{NEC}}}{k}, \\ t_{\text{k}} &= \frac{t_{\text{p}}}{2} - t_a. \end{aligned}$$

The period t_p depends on a constant parameter k and a time value that is adjusted to common to other cycles

like the NEDC period time. After the trapezoid period constant speed is held for t_0 seconds. The parameter t_0 depends on the traffic density which is expressed through ϵ_t and is defined with $0 < \epsilon_t < 1$. Depending on ϵ_t the shape of the driving cycle can be changed from a "Stop and Go" characteristic to a typical "urban" characteristic, see Fig. 3.

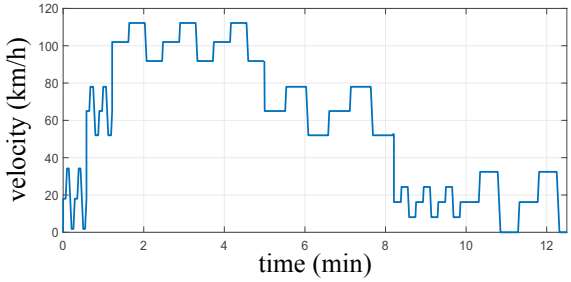

Fig. 3 Generated speed profile for different street types.

The parameters of the reference vehicles Nissan Leaf, CITROEN Berlingo, Mitsubishi I-MiEV and Mercedes Benz A-Klasse E-Cell have been utilized to generate a generic EV model, [10]. The individual parameters allow to shape the trapezoid for different traffic, driver aggressiveness, streets type or even geographic characteristics and thus to achieve an adequate consumption. To generate realistic consumptions three streets types are shaped and fitted to the data of the consumption study, [10], see Fig. 4.

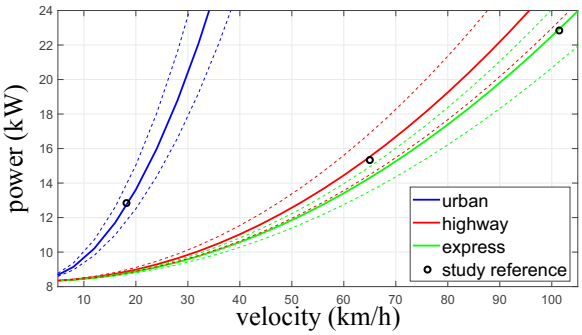

Fig. 4 Power requirement depending on street type and velocity.

With these three different types of consumptions for urban, highway and express way, the traffic and behavior parameters a individual driving cycle, see Fig. 3 can simply designed for any desired delivery routes.

2.3. Auxiliary and comfort consumers

The energy consumption P_{aux} for auxiliary consumers as radio and lights and comfort consumers as the heating and air conditioning are taken into account with an average value from the reference data, [10]. For auxiliary consumers, the mean value over the measuring points is calculated and the value of 0.4 kW is used for the simulation. It is assumed that this consumption can also be used as a good approximation for the delivery vehicle. For the comfort consumers the energy consumption depending on the ambient temperature ϑ_{amb} and the reference data is calculated. The measuring points are linearly interpolated for the heating and cooling area in order to estimate the consumption for all temperatures.The cabin temperature is kept at 20°C at different outside temperatures (-10°C to 30°C).

3. MODEL OF THERMAL SYSTEM

The following section describes the heat flow into the CB of the electrical vehicle. Main disturbances are the heat flow through the surface, the solar radiation $\dot{Q}_{\text{sol}}$ and the door openings $\dot{Q}_{\text{door}}$ for unloading the cargo. It is assumed that the goods are always pre-cooled when loaded.

3.1. Thermal model of the cargo box

The model of the CB is described by the linear differential equation

$$mc_{\text{p}} \frac{d\vartheta_{\text{CB}}}{dt} = \dot{Q}_{\text{z}} - \dot{Q}_0, \tag{9}$$

with the total thermal capacity mc_{p} of the cargo box including the content. The cooling capacity $\dot{Q}_0$ is caused by the refrigeration unit (RU) and compensates the disturbances $\dot{Q}_{\text{z}}$ which are described as follows:

$$\dot{Q}_{\text{z}} = \dot{Q}_\alpha + \dot{Q}_{\text{sol}} + \dot{Q}_{\text{door}}. \tag{10}$$

The heat flow through the surface $\dot{Q}_\alpha$ depends on the surface area A of the CB, the heat transfer coefficient of the wall α and the temperature difference of ϑ_{amb} and ϑ_{CB}:

$$\dot{Q}_\alpha = \alpha A(\vartheta_{\text{amb}} - \vartheta_{\text{CB}}). \tag{11}$$

The heat flows and their directions, Eqs. (9) to (11), act contrary to $\dot{Q}_0$, see Fig. 5. It is assumed that all heat

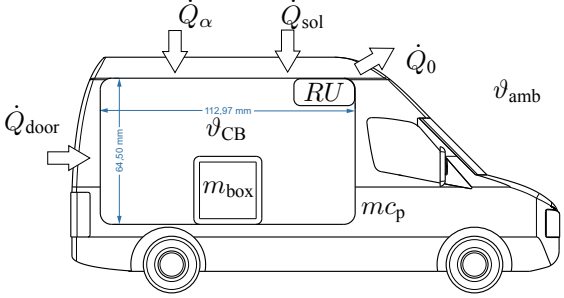

Fig. 5 Model of the cargo box and the heat flows

flows that are caused by the disturbances Q_z will be fully balanced through the RU. Also package material of the goods is not considered.

To design ϑ_{amb} depending on the time of the day weather prediction data are used. A simple approach that has been tested is to use a sine-function x_{arc}, as approximation. In this way the temperature is represented as a curve during one day with the following equations:

$$x_{\text{arc}} = \sin\left((hr - 8)\frac{\pi}{12}\right),$$

$$\vartheta_{\text{amb}} = \frac{\vartheta^{+}_{\text{amb}} + \vartheta^{-}_{\text{amb}}}{2} + \frac{\vartheta^{+}_{\text{amb}} - \vartheta^{-}_{\text{amb}}}{2} x_{\text{arc}},$$

where hr is the hour of the day and $\vartheta^{+}_{\text{amb}}$ / $\vartheta^{-}_{\text{amb}}$ the extreme values of the temperature of the day. The maximal values can vary especially during the seasons. The

energy consumption of the RU can be calculated with

$$P_{\text{el,RU}} = \frac{1}{\eta_{\text{RU}}} \dot{Q}_0 \tag{12}$$

where η_{RU} represent the efficiency factor for the RU.

3.2. Modeling the door openings

A huge impact of the energy consumption for the cargo box is the door opening during the unloading process. The value is hard to predict and depends on several parameters like, the wind speed, temperature difference between ϑ_{amb} and ϑ_{CB}, door size and duration time of the opening.

To predict the heat input during a door-opening the results of [15] are used. In this paper experiments on the infiltration heat load during door-opening of a refrigerated truck are presented. The data are adapted to the dimension of the CB and can be seen in Fig. 6.

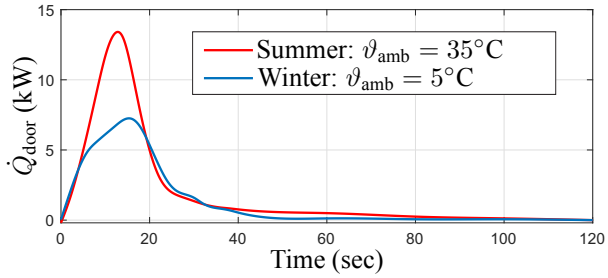

Fig. 6 Heat flow depending on infiltration rate

3.3. Solar irradiation model

The effect of solar irradiation can be divided into direct and defuse irradiation. In the model which is described in this paper, only direct irradiation is considered. To describe the position of the sun the exponential law of absorption is used, [16],

$$S(h_{\text{sun}}) = S_0 \exp\left(-\frac{B}{\sin h_{\text{sun}}}\right). \tag{13}$$

It depends on the altitude of the sun h_{sun}, the solar constant S_0 and the parameter B which depends on the season and the concentration of dust and water in the atmosphere. To calculate the altitude h_{sun} depending on the latitude χ of the chosen location following description is used

$$h_{\text{sun}} = \arcsin(\sin\chi \sin\delta - \cos\chi \cos\delta \cos\left(360° \frac{hr}{24}\right). \tag{14}$$

With the exponential law of absorption radiation, Eq.(13), and the roof surface of the vehicle A_r the radiant power $\dot{Q}_{\text{sol,r}}$ is calculated through the equation

$$\dot{Q}_{\text{sol,r}} = \kappa^{\star} A_{\text{r}} S(h_{\text{sun}}) \sin\beta, \tag{15}$$

where $\kappa^{\star}$ is the absorption coefficient and β the corresponding angle between the horizontal roof surface to the sun. The heat flow absorbed by the side areas A_s and the back are A_b of the vehicle is given by

$$\dot{Q}_{\text{sol,s}} = \kappa^{\star} (2A_s + A_b) S(h_{\text{sun}}) \frac{1}{\pi} \cos\beta. \tag{16}$$

The surface absorbs only for angles -90 $< \beta <$ 90 radiant power, otherwise it is in the shade. Also, the front surface is covered by the driver's cab, and thus is not illuminated by the sun.

The total absorbed heat flow that is caused by the solar radiation is given through

$$\dot{Q}_{\text{sol}} = \left(\dot{Q}_{\text{sol,r}} + \dot{Q}_{\text{sol,s}}\right) \cdot b_{\text{sh}}, \tag{17}$$

with $0 < b_{\text{sh}} < 1$ being a shadow parameter which can be adjusted depending on the specific location.

4. SIMULATION RESULTS

The simulation tool combines the models from Section 2 and Section 3 to calculate the required energy consumption for a chosen delivery route. Fig. 7 shows the simulation framework.

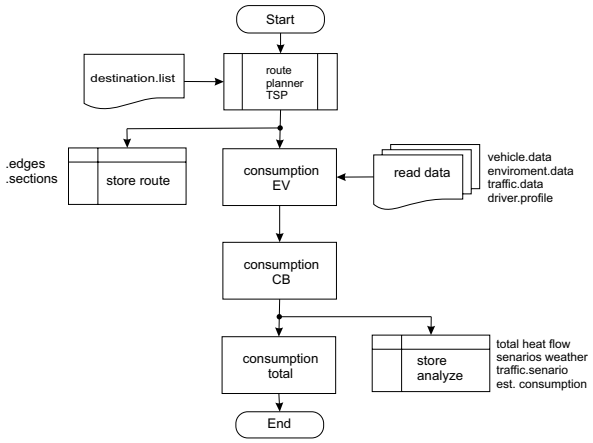

Fig. 7 Simulation framework architecture

As shown in Fig. 7 the simulation accepts data of the path between the destinations that is given by a route planner. The route planner solves the Traveling Salesman problem and gives the shortest distances between the destination points. The route is created as round trip and ends at the starting point. An interface includes the data and parameter for the vehicle and thermal model. The parameters that are used in the simulation are shown in Tab. 1. Data in Tab. 1 are specified for a generic truck. The parameter values represent mean values from 3 different manufactures.

In general, for each energy consumer an average consumption is simulated. For the simulation it is assumed that the thermal model is in steady state, therefore, the temperature in the cargo box is constant over the simulation time (ϑ_{CB} =const). It is also assumed that the RU is able to compensate all disturbances $\dot{Q}_{\text{z}} = \dot{Q}_0$.

In Fig. 8 an example route that starts at 09:00 and ends around 13:00 with eight destination points is simulated.

Table 1 Simulation parameters

	Parameter	value	unit
vehicle mass	m	1680	kg
mass vehicle	m_{cargo}	550	kg
drag coefficient	c_d	0.329	$-$
rolling coefficient	c_r	0.012	$-$
thermal capacity	cp	2.3	$\frac{J}{kgK}$
volume cargo	V	8	m^3
thermal conductivity	α	2.172	$\frac{W}{mK}$
roof surface	A_{r}	8	m^2
side surface	A_{s}	4.182	m^2
back surface	A_{b}	3.12	m^2
frontal area vehicle	A_f	4.27	m^2

The comparison of the energy consumption for the refrigeration unit, the comfort consumers and the total consumption of the delivery route over the time of the day can be seen.

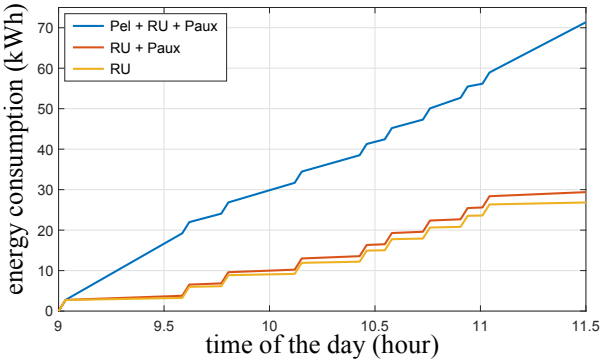

Fig. 8 Energy consumption over time for a delivery route.

For the auxiliary consumers the linear interpolation of the Tab. 2 was used, as described in Section 2.3.

Table 2 Energy auxiliary for stationary temperatures

Temperature	-20	-10	0	10	20	30
Energy [kW]	4.2	3.2	2.3	0.9	0	0.6

Fig. 9 show the comparison of the energy consumption depending on the driver aggressiveness and the season of the year.

The auxiliary and comfort consumers as the heater consume around 12-18 % of the energy during the winter season while the RU is supported by the low outside temperature. This picture is nearly the opposite during summer when the outside temperature is high which requires more energy for the RU. In comparison the heating in winter is worse than the cooling in summer. Also seen in Fig. 9, is the feature of the simulation to change the driver behavior parameter. As seen a thoughtful and predictive driver can save energy while a aggressive driver will cost 10-12% more energy.

To simulate and compare the traffic scenarios Fig. 10 shows a constant speed trip on the highway with and without traffic for different seasons.

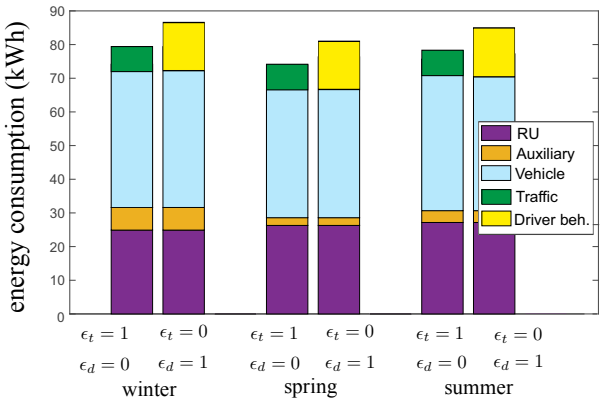

Fig. 9 Comparison seasons / traffic / driver aggressiveness

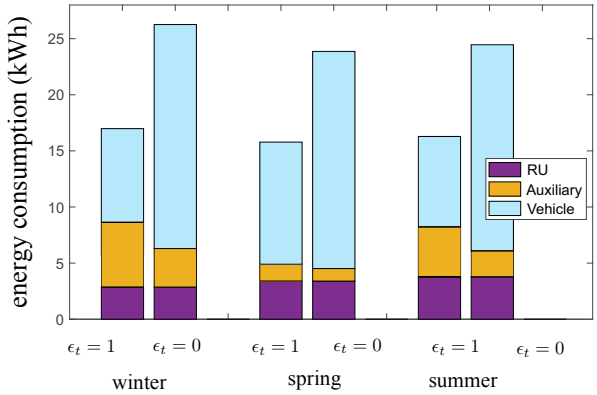

Fig. 10 Comparing constant velocity with varying the traffic parameter and seasons ($\epsilon_d = 0$)

While the energy consumption for the vehicle dynamics on high speed is the main factor, the consumption of the auxiliary consumers and the RU becomes as important as the consumption for travel.

As seen in the simulation the maximum speed during a delivery route is an important factor for the energy consumption. Therefore, the following comparison that is shown in Fig. 11 examines which velocity gives the best compromise between energy consumption for the vehicle and energy consumption for the auxiliary consumers and the RU. Fig. 11 shows that the constant speed of 40 km/h

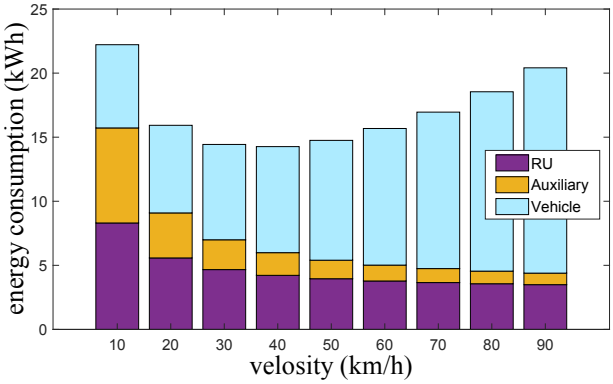

Fig. 11 Comparing different constant velocities on highway

is the optimal working point for the vehicle with CU.

5. CONCLUSION

The present study investigated the applicability of electric vehicles for the distribution of cooled goods. A framework for a simulation of the energy consumption was developed. The framework included both, the electrical vehicle and the refrigeration unit. This simulation can be used flexible to give first impressions of the needed energy of the system for different use cases. For the logistics it can be used to plan and optimize their routes which will be even more important when a EV is used. Also, it is possible to do the first design of the necessary battery capacity. As it was shown in this paper, the proposed simulation framework is flexible parameterized for different simulation scenarios. This paper showed the imported role of the refrigerating unit as an energy consumer with a electric truck. Furthermore, despite the flexibility of the presented framework, further investigations will be necessary in the future specially to find the optimal operating strategy of the whole power management system with all included energy consumers.

ACKNOWLEDGEMENTS

The authors wish to thank PRODUCTBLOKS GmbH in Korneuburg, Austria. This work was supported by the project “CONSERVE” (FFG, No. 21860205) in cooperation with PRODUCTBLOKS GmbH.

REFERENCES

[1] Directorate-General for Mobility and Transport European Commission directorate-general for mobility and transport, https://ec.europa.eu/transport/themes/urban/cts_en, accessed: 04.11.2019.

[2] W. Aggoune-Mtalaa, Z. Habbas, A. Ait Ouahmed, D. Khadraoui, Solving new urban freight distribution problems involving modular electric vehicles, IET Intelligent Transport Systems 9 (6) (2015). doi:10.1049/iet-its.2014.0212.

[3] P. Lebeau, C. De Cauwer, J. Van Mierlo, C. Macharis, W. Verbeke, T. Coosemans, Conventional, hybrid, or electric vehicles: Which technology for an urban distribution centre?, The Scientific World Journal (01 2015). doi:10.1155/2015/302867.

[4] A. Fotouhi, N. Shateri, D. J. Auger, S. Longo, K. Propp, R. Purkayastha, M. Wild, A matlab graphical user interface for battery design and simulation; from cell test data to real-world automotive simulation, 2016.

[5] J. Hayes, K. Davis, Simplified electric vehicle powertrain model for range and energy consumption based on epa coast-down parameters and test validation by argonne national lab data on the nissan leaf, 2014, pp. 1–6.

[6] A. Fotouhi, D. Auger, K. Propp, S. Longo, Simulation for prediction of vehicle efficiency, performance, range and lifetime: A review of current techniques and their applicability to current and future testing standards, 2014. doi:10.1049/cp.2014.0959.

[7] P. Cubon, J. Sedo, R. Radvan, J. Stancek, P. Spanik, J. Uricek, Calculation of demand of electric power of small electric vehicle using matlab gui, in: 2014 ELEKTRO, 2014, pp. 149–153.

[8] E. Luchini, D. Radler, D. Ritzberger, S. Jakubek, M. Kozek, Model predictive temperature control and ageing estimation for an insulated cool box, Applied Thermal Engineering 144 (2018) 269–277.

[9] S. James, C. James, J. Evans, Modelling of food transportation systems–a review, International Journal of Refrigeration 29 (6) (2006) 947–957.

[10] B. GERINGER, W. TOBER, Batterieelektrische fahrzeuge in der praxis : Kosten, reichweite, umwelt, komfort. studie des Österreichischen vereins für kraftfahrzeugtechnik und des Österreichischen automobil-, motorrad und touring clubs, ÖVK and ÖAMTC (2012).

[11] Datasheet Voltia Van electrical vehicle voltia automotive s. r. o., https://www.voltia.com/storage/document/Voltia_Van_Datasheet_EN.pdf, accessed: 05.11.2019.

[12] E. Grunditz, Design and Assessment of Battery Electric Vehicle Powertrain, with Respect to Performance, Energy Consumption and Electric Motor Thermal Capability, Chalmers, Energy and Environment, Electric Power, 2016.

[13] K. Haken, Grundlagen der Kraftfahrzeugtechnik, Hanser eLibrary, Carl Hanser Verlag GmbH & Company KG, 2015.

[14] R. Nicolas, The different driving cyclescar-engineer the different driving cycles, https://www.car-engineer.com/the-different-driving-cycles/, accessed: 05.11.2019.

[15] T. L. de Micheaux, M. Ducoulombier, J. Moureh, V. Sartre, J. Bonjour, Experimental and numerical investigation of the infiltration heat load during the opening of a refrigerated truck body, International Journal of Refrigeration 54 (2015) 170–189.

[16] Roozbeh, Ashrae fundamentals handbook 2001, kapitel 30 (2001).